Finite Element Analysis of the Deformation Distribution During Multi-Pass Rotary-Die ECAP

Y.C. Yuan, A.B. Ma, J.H. Jiang, and D.H. Yang

Rotary-die equal channel angular pressing (RD-ECAP) is a specially designed continuous processing technique to prepare bulk ultrafine-grained/nanostructure (UFG/NS) materials. In this article, an Al-7wt.% Si-0.35wt.% Mg alloy was processed by up to four RD-ECAP passes. The deformation behavior was studied by experiments and FEM simulation, including the observation of the scribed deformation patterns, the macrostructures, the simulated flow lines feature, and the equivalent stain distribution after different RD-ECAP passes. The results show that the shear deformation can accumulate effectively all over the entire billet via multi-pass RD-ECAP. The observed zigzag shape metal flow is formed after three ECAP passes, and the structure homogeneity can be achieved by RD-ECAP with more processing passes.

1. Introduction

Equal channel angular pressing (ECAP), initially developed by Segal and his colleagues (Ref 1, 2), is a severe plastic deformation (SPD) process, which is an efficient approach to produce ultrafine-grained (UFG) metals. The microstructures and corresponding mechanical properties of a metal after ECAP processing have been extensively investigated (Ref 3–7). Furthermore, the finite element method (FEM) has been applied to reveal the deformation process of a metal during ECAP, which includes simulating the plastic deformation features and the effects of die geometry/friction/material properties on the metal flow and deformation uniformity (Ref 8–17). However, most of these studies are focused on simulating the process of single pass ECAP. Multi-pass ECAP is required to obtain an ultrafine bulk material and thus, it is necessary to investigate the corresponding deformation characteristics by means of FEM. In order to simulate the deformation process of multi-pass ECAP with different routes, some researchers established S-type/multi-channel die model (Ref 18–20), which are not applied during the actual multi-pass ECAP processing.

Rotary-die equal channel angular pressing has been recently developed to realize multi-pass ECAP continuously without the need for removing the billet from the die and then re-inserting it into the die for the next pass (Ref 21, 22). Ma et al. (Ref 23, 24) have investigated mechanical properties of Al-11mass% Si alloy and ZE41 Mg alloy (Ref 25) processed by RD-ECAP. The

results show that after 32 ECAP passes, impact toughness of the Al alloy increases greatly with the absorbed energy 10 J/cm^2, which is 10 times the value of as-cast alloy of 0.9 J/cm^2. For the Mg alloy, both the yield strength and the elongation increase by 120 and 75%, respectively, at room temperature,. Therefore, these results indicate that RD-ECAP is an efficient process to improve the mechanical properties of a metal and for this reason, it is necessary to investigate the deformation features during RD-ECAP process via FEM. Yoon et al. (Ref 26) have studied the plastic flow, the strain distribution, and strain hardening behavior of pure copper by means of RD-ECAP via FEM, where the length-width ratio of the billet is 50 mm/6 mm, with the friction between the billet and die not being considered. However, when the length-width ratio becomes small and the friction exists, the deformation distribution will be complex. In this study, the flow lines of the billet of Al-7wt.%Si-0.35wt.%Mg alloy during the first four passes with length-width ratio of 2 was first analyzed by FEM; then the physical grids deformation characteristics of the Al alloy and its macrostructures evolution after 1-4 RD-ECAP passes were observed; finally, the equivalent stain distribution in the billet was discussed to reveal the deformation features of the RD-ECAP.

2. Experiments

2.1 RD-ECAP Process of Al Alloy

Rotary-die equal channel angular pressing was applied to process the Al alloy in this study, and a schematic of the processing apparatus is shown in Fig. 1. The die has two crossed channels with inner corner angles (Φ) of 90° and outer corner angles (Ψ) of 0°. The billet and punch were inserted into the vertical channel sequentially (Fig. 1a), and then a force was exerted on the punch, which led to the billet being extruded into the horizontal channel (Fig. 1b). The die was then rotated 90° clockwise, which oriented the billet vertically in the same position as at the beginning of the process (Fig. 1c). This process can be repeated, and the continuous ECAP is realized.

Y.C. Yuan, A.B. Ma, J.H. Jiang, and **D.H. Yang**, College of Mechanics and Materials, Hohai University, 1 Xikang Road, Nanjing 210098, China. Contact e-mails: rachel6074@gmail.com and aibin-ma@hhu.edu.cn.

When the ECAP process was completed, the die holder was changed with the one that has a hole in the center, after which the billet could be extruded through this hole.

In this study, the cross section of the channel is 20 mm × 20 mm, and so, the corresponding cross section of the Al alloy billet was 19.5 mm × 19.5 mm. Note that the 0.5-mm difference between the billet and the channel is to accommodate the lubricant. The length of billets was processed as 40 mm according to the dimension of the die.

In order to observe the metal flow of the billet after ECAP, the billet was cut into two pieces along the longitudinal center axis. Also 4 mm square grids were scribed on the faces. During the processing, these two half billets were put into the die with the scribed planes face to face and parallel to the front view shown in Fig. 1. After different ECAP passes at 300 °C, the billets were extruded out of the die, separated into two pieces, and the surfaces with grids were observed. Note that, after two ECAP passes, the grids are too degraded to discern. Therefore, the macrostructure in this cross section was observed instead, where the observed surface was polished and then etched by 5% HF aqueous solution.

2.2 Finite Element Analysis

Finite element analysis simulation of the multi-pass RD-ECAP was carried out by means of the commercial finite element code MARC. A finite element mesh model, shown in Fig. 2, has been established to simulate the RD-ECAP process. Because it is assumed that there is no deformation in the direction perpendicular to the front view, the two-dimensional plane strain model was used. The sizes of the channels in this model are the same as the actual die channels, and the arrangement of the mesh is similar to the grids as described previously. The size of the billet is 40 mm × 20 mm, and the width of the billet is the same as the channels.

While it is not necessary to rotate the die when these processes are simulated, in the actual RD-ECAP experiments, the die has to be rotated after finishing every pressing pass because the force can only be exerted from the top of a die. In the progress of FEM simulation, there is a punch placed in each of the four channels to exert load on the billet. Thus, after the billet is extruded by the punch 1 from channel 1 to channel 2, we can control the movement of the punch 2 in the channel 2 to extrude the billet into the channel 3, and so on. Therefore, this

FEM model can simulate the multi-pass RD-ECAP process successfully.

The die and the punches were assumed rigid so that there was no deformation during the ECAP processing. The billet was supposed to possess the rigid-plastic properties following the power law model ($S = K\varepsilon^n$), where the S is equivalent stress, ε is equivalent strain, and the constants K and n were derived by fitting the true stress-strain curve derived from the compression test of the Al alloy. The friction coefficient was assumed as 0.1 on all the sliding surfaces. Automatic re-meshing was employed to prevent the elements from distorting extremely during the progress.

3. Results and Discussion

3.1 Deformation Patterns

The simulated flow lines of the mesh are usually used to reflect the metal flow, and the deformation characteristics. There have
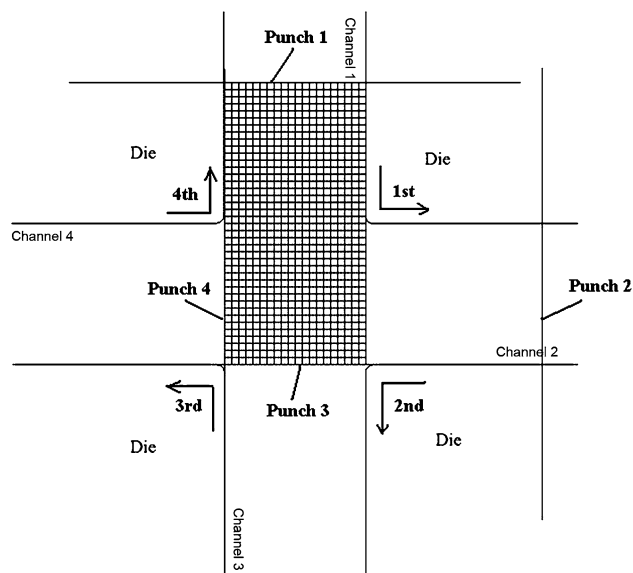

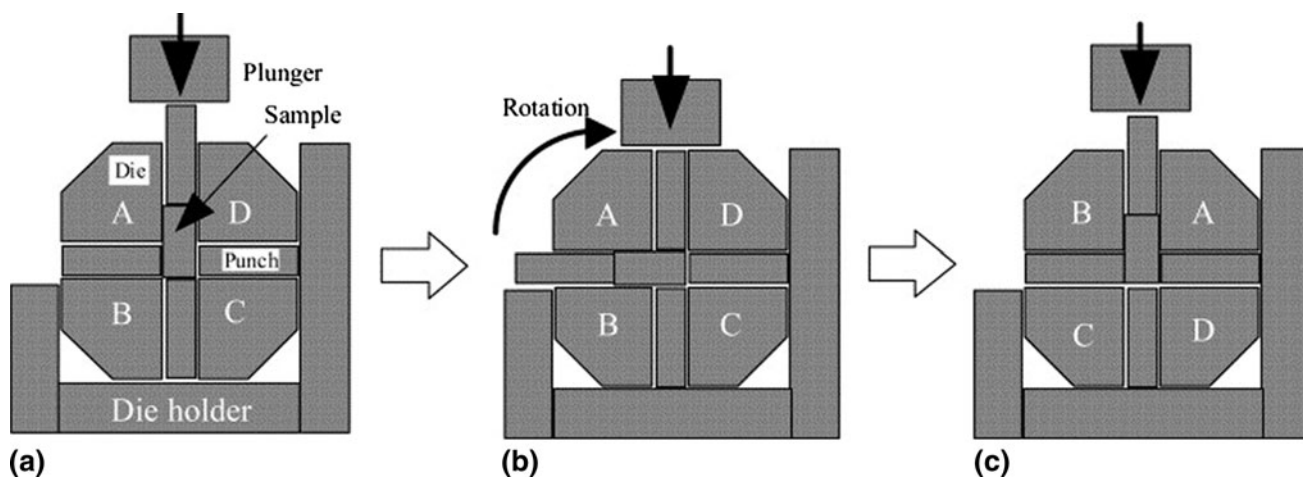**Fig. 2** Finite element mesh and the die model of RD-ECAP

Fig. 1 Schematic illustration of RD-ECAP

been several articles in the literature, describing the character of flow line patterns after single-pass ECAP process (Ref 10, 14–16, 27, 28); however, similar investigations of the flow line patterns after multi-pass ECAP process is rather limited. Figure 3 shows the mesh deformation over the whole billet with different RD-ECAP passes. Figure 3o is the original mesh before ECAP, and Fig. 3(a)-(d) represent the mesh distortion patterns with ECAP pass number of 1, 2, 3, and 4, respectively.

As shown in Fig. 3(a), there appears to be a shear zone along the shear direction after a single-pass ECAP, where the mesh deforms severely and uniformly. Note that there is almost no deformation in the mesh at the upper left and right down regions of the billet because both of these parts did not shear during the first ECAP. Furthermore, the acute outer angle ($\Psi = 0°$) (Ref 8, 11) and friction between the billet and the die (Ref 27) can hinder the metal passing through the channel corner. Thus, an extremely distorted mesh part is found at the left bottom corner as marked by the circle in Fig. 3(a).

In the second ECAP process, the "front" (part B) and "rear" (part A) parts of billet during the first ECAP process will be changed into the "rear" and "front" parts, respectively. Therefore, the shear direction in the second ECAP process (Fig. 3b) is perpendicular to that in the first ECAP as shown in Fig. 3(a). Also, the sheared zone is perpendicular to that in the

first ECAP process. In view of above reasons, the shear deformation of the mesh in different parts of the billet accumulated unequally. The mesh in the center deformed more severely, because the shear deformation in the center is high in every pass. The acute outer angle and friction can still lead to a new severe mesh deformation part as mentioned in the first ECAP process, which appears in the upper left region as marked by the circle in Fig. 3(b). In addition, the mesh which do not undergo much deformation during the first ECAP are considerably distorted, and the mesh in the upper right and left down regions of billet in Fig. 3(b) also get deformed although there is no shear deformation in the second ECAP process.

During the following ECAP process, the shear zone formed in the third ECAP process is perpendicular to the one formed in the second ECAP, and furthermore, the shear zone formed in the fourth ECAP is perpendicular to the one formed in the third ECAP. Therefore, as shown in Fig. 3(c) and (d), the extremely distorted mesh in the center produce a zigzag shape that is caused by the shear deformation accumulated after the third or fourth ECAP process. This type of shear deformation also accumulates in the other parts of billet. In addition, the mesh at the edge of the billet significantly become deformed. This is caused by the acute outer angle and the friction, which are marked by the circles in Fig. 3(c) and (d).
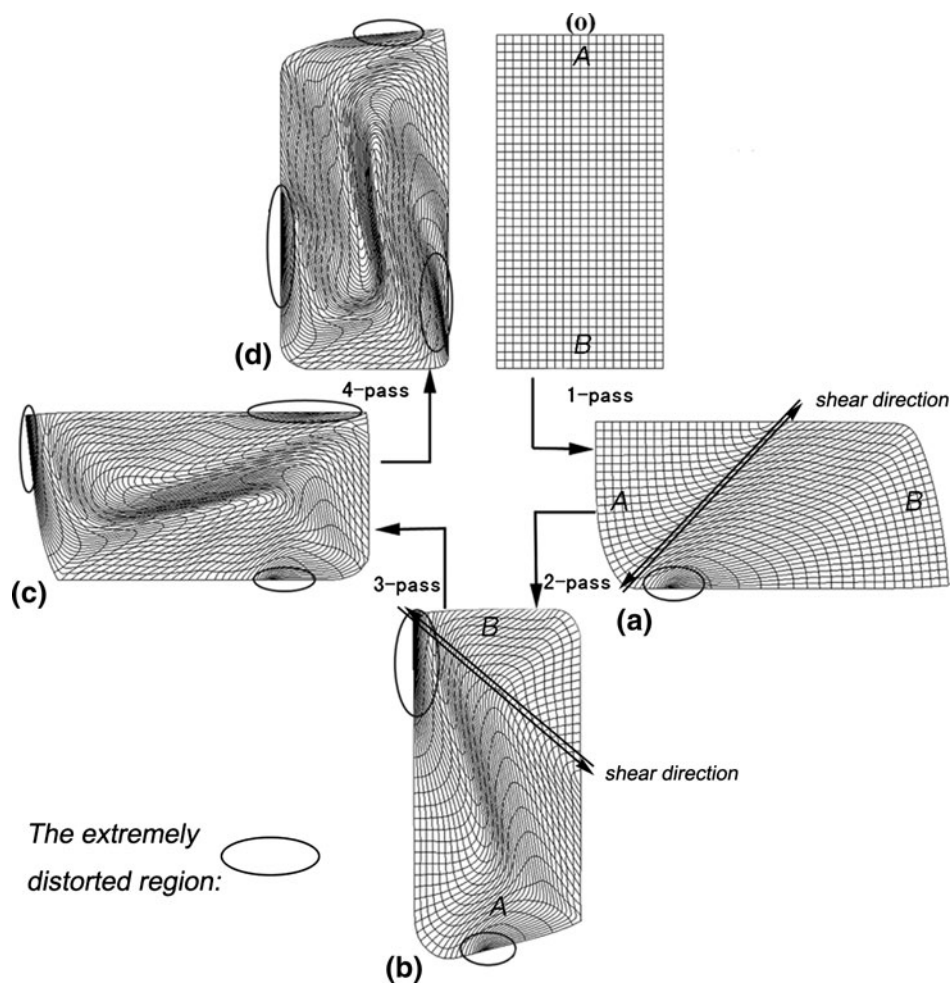

Fig. 3 The deformed grids' patterns from the section of the billet that has been extruded by RD-ECAP with (o) 0 pass, (a) 1 pass, (b) 2 passes, (c) 3 passes, (d) 4 passes

3.2 Macrostructure Observation

The sectional images of Al alloy billets with different passes of RD-ECAP are shown in Fig. 4. Figure 4(a) shows the original grids scribed on the billet; Fig. 4(b) and (d) shows the deformation features of grids after ECAP first and second passes, respectively, and Fig. 4(c), (e), (f) and (g) shows the macrostructures of metal flows for the Al alloy with ECAP pass number of 1, 2, 3, and 4, respectively.

As shown in Fig. 4(b) and (d), the deformation patterns of grids scribed on the Al alloy billet are similar with the mesh deformation patterns simulated by FEM (Fig. 3a and b). A clear deformation zone, indicated by the white arrow in Fig. 4(a) after the first ECAP pass, is observed. The grids indicated by black arrows are not appreciably deformed because these areas did not undergo significant shear. Furthermore, the severely distorted grids shown in the circled area appear at the same location as the ones in Fig. 3(a). After two ECAP passes, all the scribed grids were severely deformed because of the shear accumulation, and the distortion patterns are quite similar to those shown in Fig. 3(b).

After the third or the fourth ECAP pass, a zigzag shape (as indicated by the white curve in Fig. 4e and f) can be observed in the middle of the billet. The metal flow patterns after three or four ECAP passes are similar to those of the distorted mesh shown in Fig. 3(c) and (d), where the metal flow twists more severely with increasing number of ECAP passes.

3.3 Equivalent Strain

The equivalent strain contour is often applied to reflect the metal deformation characteristics quantitatively. Figure 5 shows the simulated results of the equivalent strain distribution contours for the longitudinal section of the Al alloy billets with different ECAP processing passes. Figure 6 shows the relationships between equivalent strain and locations along the lines of "AB," "CD," and "EF" with different ECAP processing passes.

Figure 5(a) shows that, after one ECAP pass, the equivalent strain in the region of upper left and right bottom region are much smaller than the value in the center of the billet. As shown in Fig. 6(b) and (d), the strain values at B and E points are approximately 0.001 and 0.4, respectively, whereas the equivalent strain at the middle of line "CD" is approximately 0.8. This is because the region with lower strain undergoes less deformation. According to Fig. 5(a), a severely deformed region appears at the left bottom of the billet (as indicated by the arrow in Fig. 5a), and the corresponding equivalent strain value is about 2.3 (Fig. 6a at point A). This can be attributed to
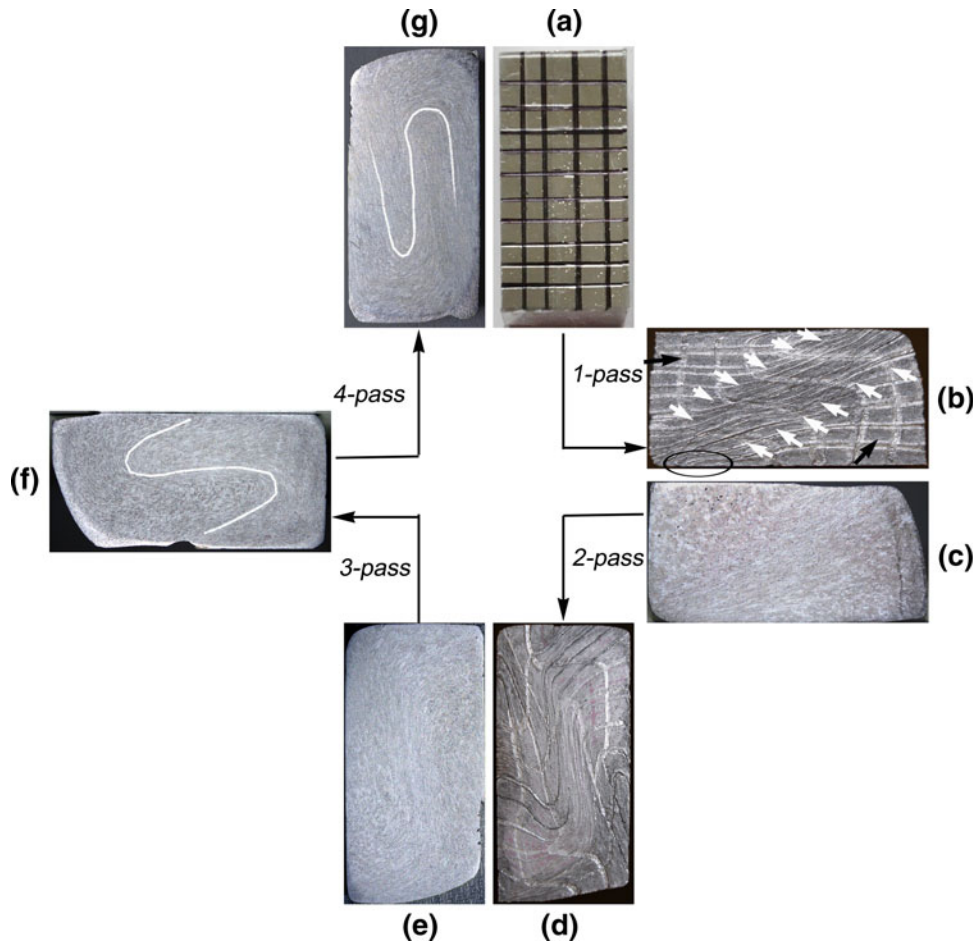

Fig. 4 The traces of scribed grids in the original billet (a), and that after extruded with (b) 1 pass, (d) 2 passes of RD-ECAP; and the macrostructure in the section of billet after extruded with (c) 1 pass, (e) 2 passes, (f) 3 passes, and (g) 4 passes
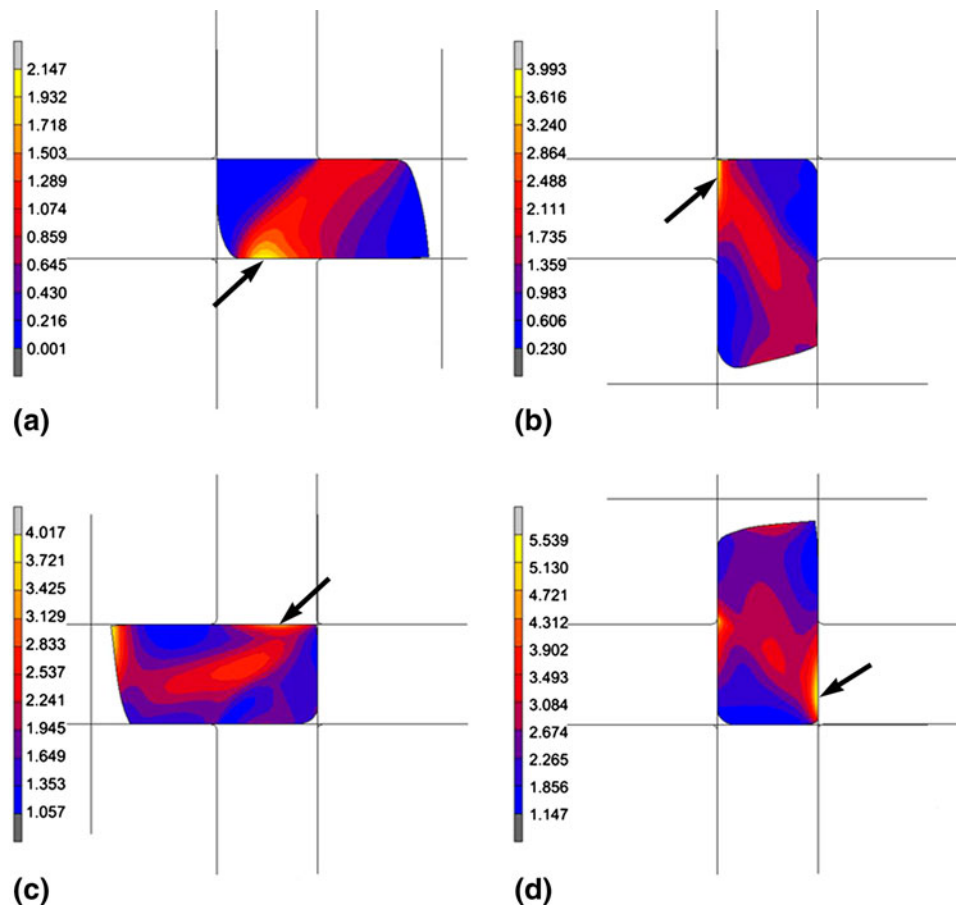
Fig. 5 The equivalent strain distributions in the section of billet after extruded (a) one pass, (b) two passes, (c) three passes, and (d) four passes of RD-ECAP

the acute angle of the outer corner and the friction between billet and die.

During the second ECAP process, the less-deformed regions produced in the first ECAP process undergo severe deformation, and the corresponding strain values increase. As shown in Fig. 6(b) and (d), the equivalent strain at both points B and E increased to approximately 0.5. Because of shear accumulation, the equivalent strain at the middle of line "CD" increased to approximately 1.7. Note that, owing to the acute angle of the outer corner and the friction between billet and die, a severely deformed region appears at the upper left location of the billet (indicated by the arrow in Fig. 5b). The corresponding equivalent strain at point A in Fig. 6(b) is about 3.5.

During the subsequent third and fourth ECAP passes, the shear accumulation causes the equivalent strain to increase over the entire billet. The acute angle of the outer corner and the friction between the billet and the die lead to the extremely high value of equivalent strain shown in Fig. 5(c) and (d) (marked by the black arrows). After four ECAP passes, the highest equivalent strain is 5.3 at point A in Fig. 6(b). The shear deformation continues to accumulate in the central region of the billet and, as such, the corresponding equivalent strain also increases. The average equivalent strain value in this region is approximately 3.5 after four ECAP passes (as shown in Fig. 6c at the middle of line "CD"). Figure 5 and 6 indicate that the equivalent strain difference among the billet becomes smaller with increasing ECAP passes. The ratio between the highest and

the lowest equivalent strain values decreases from 100 (2.14/0.21) to 2.12 (5.3/2.5) thereby indicating that the structure homogeneity can be improved with additional RD-ECAP passes.

4. Conclusions

The deformation behaviors of multi-pass rotary-die equal channel angular pressing (RD-ECAP) for Al-7wt.%Si-0.35wt.%Mg alloy have been investigated using scribed grids' deformation and macrostructure observation, and FEM simulation. The results have led us to the following conclusions: (1) During continuous multi-pass RD-ECAP, the shear direction produced during each pass is perpendicular to that formed in the last ECAP pass. Thus, shear deformation can accumulate in different parts of the billet. After four ECAP passes, the shear deformation accumulates uniformly over the entire billet. (2) An extremely deformed region is formed near the edge of the billet after every pass of ECAP, which is a result of the combined effects produced by the acute outer corner angles of the die and the friction between the die and the billet. (3) The zigzag-shaped metal flow is formed in the billet with the third and fourth passes of ECAP. The accumulated equivalent strain in the center of the billet is rather high (approximately 3.5) after four ECAP passes and the ratio of the highest to lowest equivalent values in the entire billet decreases from 1000 to
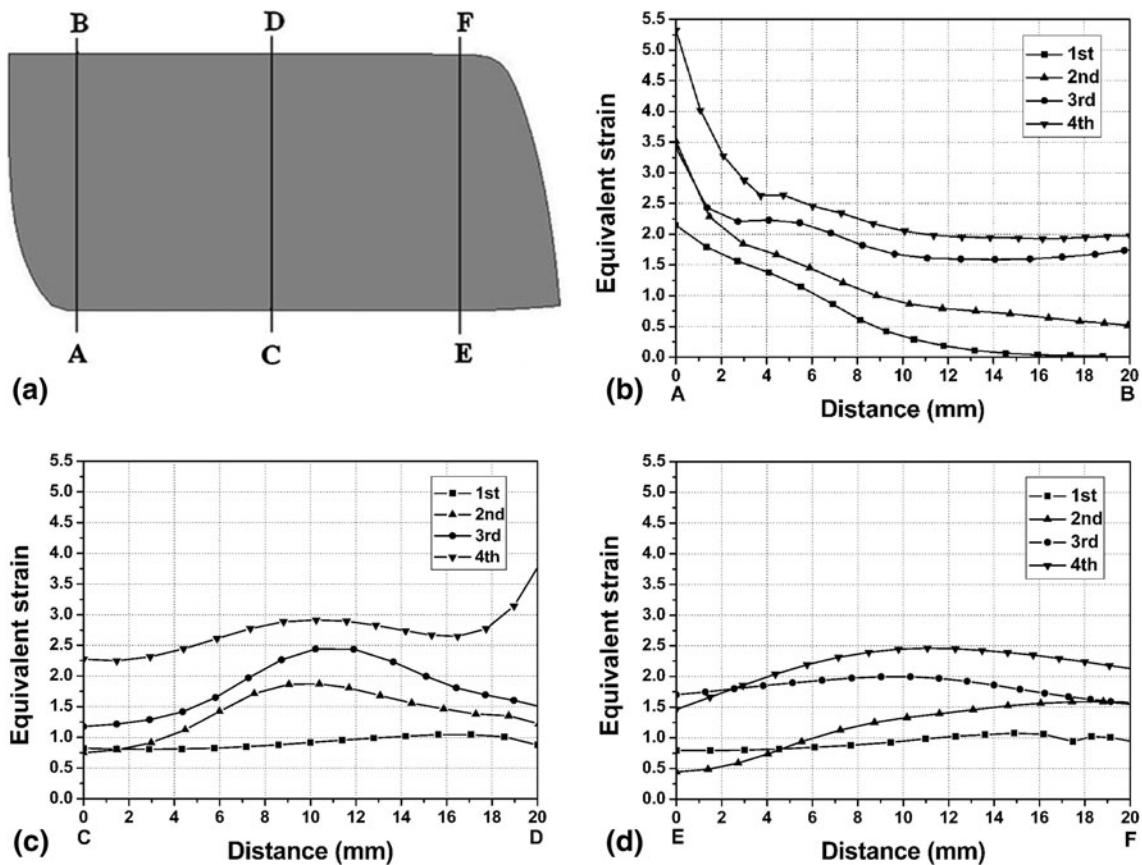
Fig. 6 The equivalent strains measured across the billet along the line of, (b) A-B, (c) C-D, and (d) E-F, which are marked in (a)

2.12, which imply that the deformation homogeneity can be improved by RD-ECAP with more passes.

References

1. V.M. Segal, Materials Processing by Simple Shear, *Mater. Sci. Eng. A*, 1995, **197**, p 157–164
2. V.M. Segal, Equal Channel Angular Extrusion: From Macromechanics to Structure Formation, *Mater. Sci. Eng. A*, 1999, **271**, p 322–333
3. Y. Iwahashi, J. Wang, Z. Horita, M. Nemoto, and T.G. Langdon, Principle of Equal-Channel Angular Pressing for the Processing of Ultra-Fine Grained Materials, *Scr. Mater.*, 1996, **35**, p 143–146
4. T.G. Langdon, M. Furukawa, M. Nemoto, and Z. Horita, Using Equal Channel Angular Pressing for Refining Grain Size, *JOM*, 2000, **52**, p 30–33
5. I.P. Semenova, G.I. Raab, L.R. Saitova, and R.Z. Valiev, The Effect of Equal-Channel Angular Pressing on the Structure and Mechanical Behavior of Ti-6Al-4V Alloy, *Mater. Sci. Eng. A*, 2004, **387–389**, p 805–808
6. Y.H. Zhao, X.Z. Liao, Z. Jin, R.Z. Valiev, and Y.T. Zhu, Microstructures and Mechanical Properties of Ultrafine Grained 7075 Al Alloy Processed by ECAP and Their Evolutions During Annealing, *Acta Mater.*, 2004, **52**, p 4589–4599
7. S. Li, A.A. Gazder, I.J. Beyerlein, C.H.J. Davies, and E.V. Pereloma, Microstructure and Texture Evolution During Equal Channel Angular Extrusion of Interstitial-Free Steel: Effects of Die Angle and Processing Route, *Acta Mater.*, 2007, **55**, p 1017–1032
8. A.V. Nagasekhar and Y. Tick-Hon, Optimal Tool Angles for Equal Channel Angular Extrusion of Strain Hardening Materials by Finite Element Analysis, *Comput. Mater. Sci.*, 2004, **30**, p 489–895
9. A.V. Nagasekhar, Y. Tick-Hon, S. Li, and H.P. Seow, Effect of Acute Tool-Angles on Equal Channel Angular Extrusion/Pressing, *Mater. Sci. Eng. A*, 2005, **410–411**, p 269–272
10. S.C. Yoon and H.S. Kim, Finite Element Analysis of the Effect of the Inner Corner Angle in Equal Channel Angular Pressing, *Mater. Sci. Eng. A*, 2008, **490**, p 438–444
11. V. Patil Basavaraj, U. Chakkingal, and T.S. Prasanna Kumar, Study of Channel Angle Influence on Material Flow and Strain Inhomogeneity in Equal Channel Angular Pressing Using 3D Finite Element Simulation, *J. Mater. Process. Technol.*, 2009, **209**, p 89–95
12. N. Medeiros, J.F.C. Lins, L.P. Moreira, and J.P. Gouvêa, The Role of the Friction During the Equal Channel Angular Pressing of an IF-Steel Billet, *Mater. Sci. Eng. A*, 2008, **489**, p 363–372
13. I.H. Son, Y.G. Jin, Y.T. Im, S.H. Chon, and J.K. Park, Sensitivity of Friction Condition in Finite Element Investigations of Equal Channel Angular Extrusion, *Mater. Sci. Eng. A*, 2007, **445–446**, p 676–685
14. R.B. Figueiredo, M.T.P. Aguilar, and P.R. Cetlin, Finite Element Modelling of plastic Instability During ECAP Processing of Flow-Softening Materials, *Mater. Sci. Eng. A*, 2006, **430**, p 179–184
15. S.L. Semiatin, D.P. DeLo, and E.B. Shell, The Effect of Material Properties and Tooling Design on Deformation and Fracture During Equal Channel Angular Extrusion, *Acta Mater.*, 2000, **48**, p 1841–1851
16. S. Li, M.A.M. Bourke, I.J. Beyerlein, D.J. Alexander, and B. Clausen, Finite Element Analysis of the Plastic Deformation Zone and Working Load in Equal Channel Angular Extrusion, *Mater. Sci. Eng. A*, 2004, **382**, p 217–236
17. S. Dumoulin, H.J. Roven, J.C. Werenskiold, and H.S. Valberg, Finite Element Modeling of Equal Channel Angular Pressing: Effect of Material Properties, Friction and Die Geometry, *Mater. Sci. Eng. A*, 2005, **410–411**, p 248–251

18. E. Cerri, P.P. De Marco, and P. Leo, FEM and Metallurgical Analysis of Modified 6082 Aluminium Alloys Processed by Multipass ECAP: Influence of Material Properties and Different Process Settings on Induced Plastic Strain, *J. Mater. Process. Technol.*, 2009, **209**, p 1550–1564

19. H.S. Kim, Finite Element Analysis of Deformation Behaviour of Metals During Equal Channel Multi-Angular Pressing, *Mater. Sci. Eng. A*, 2002, **328**, p 317–323

20. A. Rosochowski and L. Olejnik, Numerical and Physical Modelling of Plastic Deformation in 2-Turn Equal Channel Angular Extrusion, *J. Mater. Process. Technol.*, 2002, **125–126**, p 309–316

21. Y. Nishida, H. Arima, J.C. Kim, and T. Ando, Rotary-Die Equal-Channel Angular Pressing of an Al7Mass% Si-0.35Mass% Mg Alloy, *Scr. Mater.*, 2001, **45**, p 261–266

22. S. Li, I.J. Beyerlein, and M.A.M. Bourke, Texture Formation During Equal Channel Angular Extrusion of Fcc and Bcc Materials: Comparison with Simple Shear, *Mater. Sci. Eng. A*, 2005, **394**, p 66–77

23. A. Ma, K. Suzuki, Y. Nishida, N. Saito, I. Shigematsu, and M. Takagi, Impact Toughness of an Ultrafine-Grained Al-11Mass%Si Alloy Processed by Rotary-Die Equal-Channel Angular Pressing, *Acta Mater.*, 2005, **53**, p 211–220

24. A. Ma, M. Takagi, N. Saito, H. Iwata, Y. Nishida, and K. Suzuki, Tensile Properties of an Al-11Mass%Si Alloy at Elevated Temperatures Processed by Rotary-Die Equal-Channel Angular Pressing, *Mater. Sci. Eng. A*, 2005, **408**, p 147–153

25. A. Ma, J. Jiang, N. Saito, I. Shigematsu, Y. Yuan, and D. Yang, Improving Both Strength and Ductility of an Mg Alloy Through a Large Number of ECAP Passes, *Mater. Sci. Eng. A*, 2009, **513–514**, p 122–127

26. S.C. Yoon, M.H. Seo, A. Krishnaiah, and H.S. Kim, Finite Element Analysis of Rotary-Die Equal Channel Angular Pressing, *Mater. Sci. Eng. A*, 2008, **490**, p 289–292

27. J.R. Bowen, A. Gholinia, S.M. Roberts, and P.B. Prangnell, Analysis of the Billet Deformation Behavior in Equal Channel Angular Extrusion, *Mater. Sci. Eng. A*, 2000, **287**, p 87–99

28. S.C. Baik, Y. Estrin, H.S. Kim, and R.J. Hellmig, Dislocation Density-Based Modeling of Deformation Behavior of Aluminium Under Equal Channel Angular Pressing, *Mater. Sci. Eng. A*, 2003, **351**, p 86–97